Zhihao Feng

PREPARATION OF HYDROPHOBIC HKUST-1 MATERIAL AND STUDY ON ITS WATER ADSORPTION PERFORMANCE

Thesis
CENTRIA UNIVERSITY OF APPLIED SCIENCES
Degree Programme
February 2023

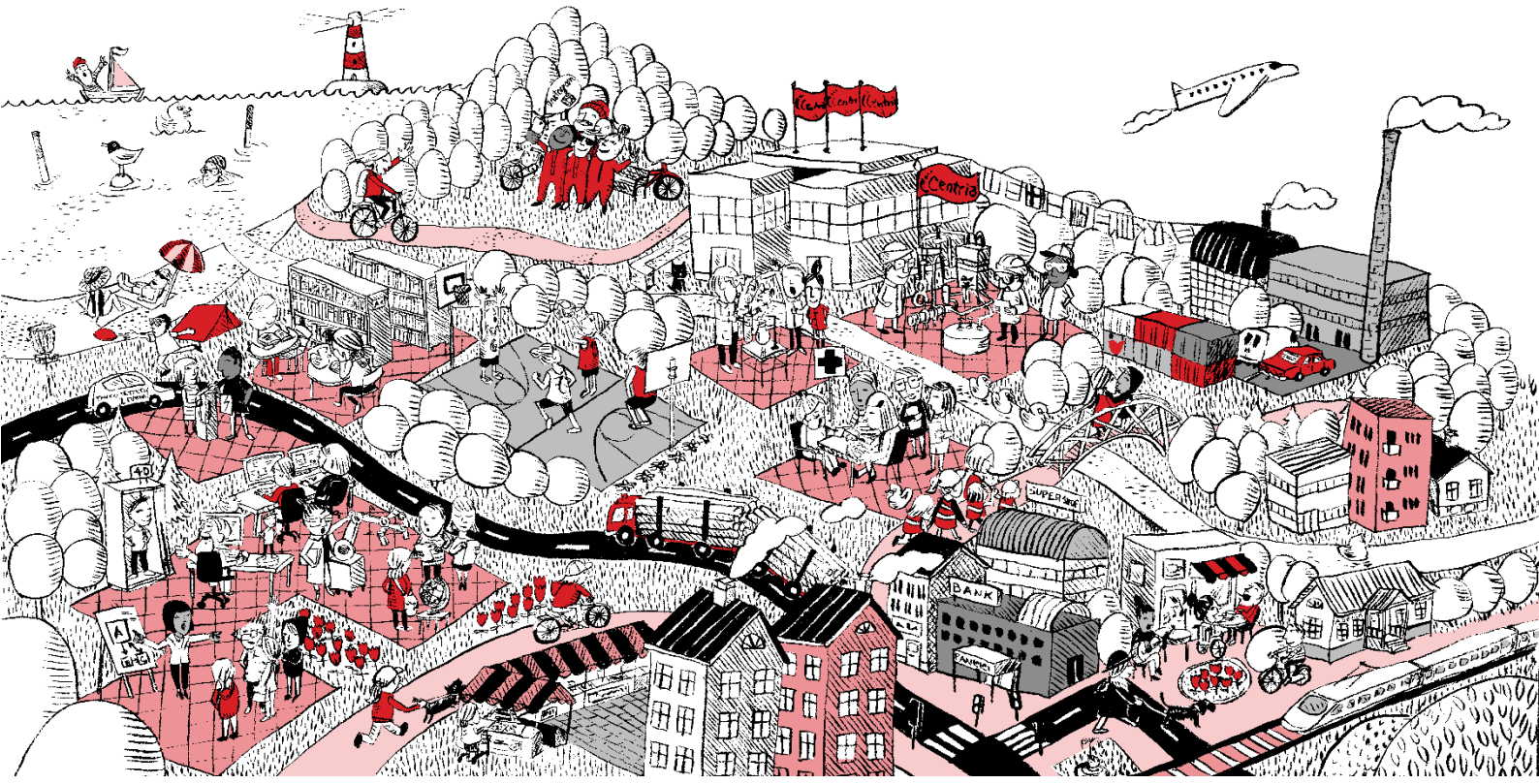

ABSTRACT

Centria University of Applied Sciences	Date February 2023	Author Zhihao Feng
Degree programme Environmental Chemistry and Technology		
Name of thesis PREPARATION OF HYDROPHOBIC HKUST-1 MATERIAL AND STUDY ON ITS WATER ADSORPTION PERFORMANCE		
Centria supervisor Yue Dong		**Pages** 30
Instructor Feng Xu		

Metal Organic Frameworks have the advantages of porosity, large specific surface area and unsaturated metal sites, and are widely used in the fields of adsorption separation, membrane separation and catalysis. However, in practical applications, due to the influence of factors such as water competitive adsorption and poor water stability, the adsorption performance of the material is considerably reduced. In response to this problem, HKUST-1 materials were quickly prepared under normal temperature and pressure, and then hydrophobically modified it to enhance the hydrophobic properties of the material. Subsequently, the water adsorption performance of the material before and after the hydrophobic modification was measured under different relative humidity conditions by gravimetric method.

The results show that the BET specific surface area of the hydrophobically modified material has changed from 1016.2 m^2/g to 904.7 m^2/g, means that it has slightly reduced. However, the hydrophobic performance has considerably improved. The left contact angle is 125.0°, and the right contact angle is 127.3°. When the relative humidity is 81%, the water adsorption capacity of the original material after hydrophobic modification is reduced from 23.7 mmol/g to 15.1 mmol/g, which is a decrease of 36.3%, and the diffusion coefficient changes from 1.88×10^{-13} cm^2/s to $1.46\times10^{-13}cm^2/s$. At a relative humidity of 32.8%, the material's water adsorption capacity decreased from 19.9 mmol/g to 14.1 mmol/g, which is a decrease of 29.1%, and the diffusion coefficient changed from 1.54×10^{-13} cm^2/s to 1.36×10^{-13} cm^2/s.

Key words
HKUST-1, hydrophobic modification, metal organic framework, water adsorption performance

CONCEPT DEFINITIONS

MOFs	Metal Organic Frameworks
BET	Brunauer-Emmett-Teller measurements
PDMS	Polydimethylsiloxane
XRD	X-ray diffraction
DMF	N-N-dimethylformamide
$CH_3(CH_2)_{15}Si(OCH_3)_3$	hexadecyltrimethoxySilane
D_M	Diffusion coefficient
TG	Thermogravimetric
CO_2	Carbon Dioxide
H_2	Hydrogen
CH_4	Methane
N_2	Nitrogen
Zn^{2+}	Zinc ions
Co^{2+}	Cobalt ions
Cu^{2+}	Copper ions
HKUST-1	1-(2-methyl-4-(2-oxopyrrolidin-1-yl) phenyl)-3-morpho-lino-5,6-dihydropyridin-2(1H)-one
HKUST-1-A	It is the material after HKUST-1 is hydrophobically modi-fied by hexadecyltrimethoxySilane.
MOF-5 or IRMOF-1	$Zn_4O(BDC)_3$, BDC= 1,4-benzenedicarboxylate
UIO-66(Zr)	University of Oslo, (1R)-1,5-Anhydro-1-C-[3-[[5-(4-fluoro-phenyl)-2-thienyl] methyl]-4-methylphenyl]-D-glucitol
ZIF-8, ZIF-11, ZIF	Zeolitic imidazolate framework
MIL-100, MIL-101	Materials of Institut Lavoisier
MOF-801, ZnBT	Some MOFs materials

ABSTRACT
CONCEPT DEFINITIONS
CONTENTS

FIGURES

TABLES

1 INTRODUCTION

Metal organic frameworks (MOFs) porous materials are zeolite-like materials with a supramolecular microporous network structure formed by self-assembly of organic ligands and metal ions through complexation. Because of its crystal structure, high permanent porosity, high specific surface area, high pore volume, and adjustable pore size and shape, it shows a good application prospect in gas storage and separation. (Wang, Mcguirk & Aquino 2018.)

MOFs are a new type of porous material, which can be designed by selecting specific components according to needs. MOFs are also the materials with the lowest density and the largest specific surface area so far. Compared with zeolite and activated carbon, MOFs generally exhibit higher pore volume and surface area. (Wang et al. 2018.) After removing the guest molecules from MOFs, many voids are left, making it a porous material. Porosity is an important feature of MOFs, which makes it widely used in catalysis (Dhakshinamoorthy, Li & Garcia 2018, 8134-8172; Ma, Lia & Shia 2018, 827-830), gas adsorption and separation (Olajire 2018, 570-607; Mukherjee, Desai & Ghosh 2018, 82-126), and chemical sensors (Fand, Zong & Mao 2018, 64-82; Wang, Lustig & Li 2018, 4729-4756).

However, in a humid environment, the adsorption performance of MOFs materials are considerably reduced due to the influence of water competitive adsorption and poor water stability. 1-(2-methyl-4-(2-oxopyrrolidin-1-yl) phenyl)-3-morpholino-5,6-dihydropyridin-2(1H)-one (HKUST-1) material is a very typical MOFs material. Therefore, the aim of this thesis work was to select HKUST-1 material for hydrophobic modification experiment to improve the adsorption performance of MOFs by improving the hydrophobicity of the material. (Burtch, Jasuja & Walton 2014, 10575-10612.)

First, a large amount of HKUST-1 raw materials must be prepared. Then the original material of HKUST-1 was hydrophobically modified, and then the material was characterized by X-ray diffraction (XRD), Thermogravimetric (TG), Brunauer-Emmett-Teller measurements (BET), infrared spectroscopy and contact angle measurement. Finally, the water absorption properties of HKUST-1 original material and HKUST-1-A hydrophobically modified material were measured.

2 RESEARCH BACKGROUND

MOFs materials are porous hybrid materials coordinated by metal ions or metal cluster centers and organic ligands (Guan, Leblanc & Xie 2018, 76-90). In the past two decades, MOFs materials have been widely reported, and increasing scientists are studying MOFs materials (Olajire 2018, 570-607; Dhakshinamoorthy et al. 2018, 8134-8172; Fand et al. 2018, 64-82). MOFs materials are used in various fields such as gas-liquid adsorption separation, membrane separation, and catalytic reactions. Compared with the previous porous materials, MOFs materials have the advantages of larger specific surface area and pore volume. (Wang et al. 2018).

By replacing the metal cluster center and the organic ligand in the MOFs material, the pore size of the MOFs material can be adjusted to have a wider pore size. Therefore, MOFs materials have potential applications in gas adsorption and separation (Olajire 2018, 570-607; Mukherjee et al. 2018, 82-126), shape-selective catalysis (Dhakshinamoorthy et al. 2018, 8134-8172; Ma et al. 2018, 827-830), drug delivery (Simon, Mielcarek & Couvreur 2018) and sensor detection (Fand et al. 2018, 64-82; Wang, Lustig & Li 2018, 4729-4756).

2.1 MOFs material application

MOFs materials have many advantages, such as ultra-high specific surface area, rich pore structure, adjustable unsaturated metal sites and pore structure. Therefore, MOFs materials also have many applications. In this section, the applications of MOFs materials are discussed in the fields of gas storage, adsorption and separation, biomedicine and luminescent materials. (Wang et al. 2018.)

2.1.1 Gas storage

MOFs materials have a pivotal position in the field of gas storage and are a very popular porous material. MOFs materials have very good properties and can be used in the field of gas storage, such as Carbon Dioxide, Hydrogen, Methane. For example, Kaye, Dailly & Yaghi (2007, 14176-14180) found that under low temperature conditions, $Zn_4O(BDC)_3$ (MOF-5 or IRMOF-1; BDC= 1,4-

benzenedicarboxylate) can store H_2 very well. Compared with all H_2 storage materials, this material has the highest storage capacity for H_2.

Yu & Balbuena (2015, 117-124) studied the adsorption and separation of CO_2 by (1R)-1,5-Anhydro-1-C-[3-[[5-(4-fluorophenyl)-2-thienyl] methyl]-4-methylphenyl]-D-glucitol (UIO-66(Zr)) material. The results show that when the material is used to adsorb a mixture of Nitrogen (N_2) and CO_2, its adsorption rate of CO_2 is much greater than that of N_2.

2.1.2 Adsorption and separation

The adsorption and separation process of MOFs materials for gas is completed by the adsorption and desorption of a certain gas in the gas mixture. Therefore, if a certain gas is to be separated from the mixed gas, there must be different interactions between the gas and other gases and the frame, which can be size or power. Only then can the gas be separated. (Zhang & Gao 2018, 53-57.)

Ke, Peng & Zhang (2018, 1-11) found that when MOF-801 material is used to extract fluoride from brick tea, it has a good effect. Specifically, at room temperature, 80% of the fluoride in brick tea can be extracted within five minutes, while the content of tea and caffeine remains basically unchanged. This also illustrates the feasibility of using MOFs to selectively extract fluoride in brick tea.

2.1.3 Biomedicine

In addition to the advantages of high specific surface area, MOFs materials also have high drug loading. In the biomedical research of MOFs materials, some MOFs materials have been found to have excellent properties in the field of nanomedicine, which provides a new method for the development of new nanoscale therapeutic drugs. For example, some materials have a pore size just enough to allow cancer drugs and other molecules to enter the pores, allowing the drug to be transported. In simple terms, MOFs can be used as a carrier medium, which can be visually understood as a trolley for delivering goods, delivering the correct drug (goods) to the correct destination accurately, safely and efficiently, such as target organs, target cells and target tissues. (Patricia, Serre & Vallet-Regí 2006, 5974-5978.)

Patricia et al. (2006, 5974-5978) reported for the first time the carrying capacity and delivery capacity of Materials of Institut Lavoisier (MIL-100 and MIL-101) materials for ibuprofen. They also emphasized the great potential for the development of new MOFs materials, including the benefits of adapting to drug structure and dosage requirements.

2.1.4 Luminescent materials

Solids that emit light when excited by the outside world are called luminescent materials. When a substance is excited (rays, high-energy particles, electron beams and external electric fields), the substance will be in an excited state, and the energy of the excited state will be released in the form of light or heat. If this part of the energy is electromagnetic radiation in the visible, ultraviolet or near-infrared, the process is called luminescence. Luminescent materials have a wide range of applications in the fields of lighting, organic pigments and drug tracers. MOFs materials have excellent performance in the field of luminescence, because their organic and inorganic parts can have luminous effects (Binnemans 2009, 4283-4374). In addition, MOFs materials can also inherit electronic and optical properties (Zhang, Wang & Li 2017, 1-9; Wang, Li & Li 2017, 1-9).

For example, Gao, Yang & Ai (2016, 11652-11659) discovered a MOFs material that contains manganese, which can quickly adsorb and decompose methyl orange dye, and also has a good light-to-light discoloration effect. When the material is exposed to visible light at room temperature, the color of the material changes from light yellow to green. (Gao et al. 2016, 11652-11659).

However, the actual use of MOFs materials are still very limited so far. One of the most important reasons is that the stability and adsorption capacity of MOFs materials in a humid environment will be considerably reduced (Burtch et al. 2014, 10575-10612). One of the reasons for this phenomenon is that the strongly polar water will attack the metal clusters and then coordinate with them, and change the pore structure of the MOFs material, thereby reducing the adsorption capacity of the target molecules (Howarth, Liu & Li 2016, 1-15). Another important reason is that although the frame structure of MOFs materials is relatively stable with respect to water, MOFs materials have the ability to adsorb water at the empty coordination sites in the metal center. Therefore, in a humid environment, competitive adsorption will also reduce the adsorption capacity of MOFs to target molecules (Canivet, Fateeva & Guo 2014, 5594-5617). Therefore, improving the hydrophobicity and water stability of MOFs

materials through reasonable process control and material changes will help promote the application process of MOFs materials (Mon, Bruno & Ferrando 2018, 4912-4947).

2.2 MOFs material hydrophobic modification

Taddei, Costantino & Vivani (2016, 4300-4309) have researched many the hydrophobic modification of MOFs materials, and have achieved good modification effects. The modification process described so far can be roughly divided into the hydrophobic modification of the material surface coating method, the hydrophobic modification of the main structure of the material, and other modification methods (Duan, Jin & Kitagawa 2017, 48-74). The material surface coating method is to coat the outer surface of the material with a hydrophobic material, and use the hydrophobic effect of the hydrophobic material to improve the hydrophobic performance of the MOFs materials. The hydrophobic modification of the main structure of the material is through the selection of a specific metal center and ligand to obtain MOFs with strong coordination (Ferey, Mellot & Serre 2005, 2040-2042), or by modifying the organic ligand to add hydrophobic alkane on the ligand (Yang, Kaipa & Mather 2011, 18094-18097). They have a strong binding ability. Therefore, MOFs with better hydrophobic effect can be produced. In addition, the hydrophobicity of MOFs can be improved by combining hydrophobic materials with MOFs or other modification methods (Mustafa, Breynaert & Bajpe 2011, 8037-8039; Sun, He & Gao 2011, 13300).

2.2.1 Hydrophobic modification of MOFs material surface coating method

The hydrophobic MOFs materials are prepared based on the direct synthesis method or the ligand modification method. Although materials with excellent hydrophobicity can be obtained, the manufacturing process is complicated and will affect the pore structure of the MOFs materials. It usually has a significant impact on the pore structure and specific surface area of the material, thereby affecting the performance of the material. The surface coating method uses a hydrophobic substance to coat the surface of the MOFs material, which gives the MOFs material excellent hydrophobicity, and the surface coating has little effect on the structural properties of the material (Fernandez, Nune & Annapureddy 2015, 13490-13497).

In the study of coating MOFs with hydrophobic reagents (Merkel, Bondar & Nagai 2000, 415-434), polysilanes with high chemical stability, non-toxic and odorless, have become widely used hydrophobic reagents due to their high hydrophobicity and easy coating on the surface of MOFs materials. Among them, polydimethylsiloxane (PDMS) is highly hydrophobic, which can effectively prevent the adsorption of water vapor by MOFs. Its porous structure can also promote the penetration and diffusion of gas molecules into the material, and can pre-enrich low-density gases well. In addition, PDMS is a non-polar material and follows the principle of similar compatibility. Therefore, PDMS can improve the adsorption selectivity of the same non-polar organic gas. Consequently, PDMS is widely used for hydrophobic modification of MOFs and other materials. (Merkel et al. 2000, 415-434.)

In a closed container at 235 ℃, Zhang, Hu & Ge (2014, 16978-16981) used a high-temperature coating method to coat the surface of MOFs such as HKUST-1, ZnBT, and MOF-5 with a hydrophobic reagent. At 235 ℃, most MOFs materials can retain their crystalline form. PDMS decomposes the vapor of silicon-containing compounds at this temperature, and then gradually deposits on the surface of MOFs materials, and then re-polymerizes to form a hydrophobic coating. The coated MOFs material not only retain the crystal structure and pore structure characteristics of its predecessor, but also retain 100% of the specific surface area. This hydrophobic modification method can considerably improve the practicability of MOFs under humid or high humidity conditions. (Zhang et al. 2014, 16978-16981.)

2.2.2 Hydrophobic modification of the main structure of MOFs

The influence of water on MOFs materials is mainly reflected in the destruction of the coordination bonds of MOFs materials and the occupation of the adsorption centers of MOFs materials. The hydrophobic modification of the main structure of MOFs materials mainly uses the hydrophobicity of the organic groups in the ligands, the steric hindrance effect of the organic groups, and the enhancement of the coordination bond strength between the metal center and the organic ligands. (Burtch et al. 2014, 10575-10612.)

MOFs materials can be modified by hydrophobic organic group modification. According to the principle of similar compatibility, non-polar or weakly polar organic groups are incompatible with polar water molecules. Since the organic groups of the MOFs ligand can be modified to form a hydrophobic

organic framework, water molecules cannot penetrate the metal center of the framework material, which will not affect the structural stability and adsorption capacity of the material. The methods currently used mainly include increasing the length of the organic chain of organic ligands and using hydrophobic fluorine-containing ligands. (Zhang 2021, 61-66.)

For example, Zeolitic imidazolate framework (ZIF-8, ZIF-11 or ZIF) material is a kind of MOFs material that is easily hydrolyzed in contact with water. Liu, Li & Ban (2013, 9140-9142) adopted a shell ligand exchange method, only using the sieving effect of the ZIF-8 material pores, using dimethyl benzo. The imidazole ligand replaced the imidazole ligand on the surface of the ZIF-8 material, which successfully enhanced the hydrophobicity and water stability of the ZIF-8 material. While enhancing the water stability of the material, it does not affect the performance, but also enhances the membrane separation performance and adsorption performance of the material, and avoids the influence of organic ligands on the pore properties and adsorption performance of the material. (Liu et al. 2013, 9140-9142.)

MOFs materials can also be hydrophobically modified by enhancing the strength of coordination bonds. The soft, hard acid and base theory can be used to assemble specific metal ligands and different types of organic ligands to obtain MOFs with high-strength coordination bonds. The principle of soft and hard acid-base theory is that the soft acid that carries a small number of positive charges will produce stronger ligands when it is coordinated with the soft base; the hard acid that carries a high number of positive charges is hard acid, which is coordinated with the hard base. Position binding will produce stronger ligands. (Pearson 1963, 3533-3539.)

Based on this principle, Park, Ni & Cote (2006, 10186) used nitrogen-containing ligand imidazole to react with divalent metal ions such as Zinc ions (Zn^{2+}) or Cobalt ions (Co^{2+}) to synthesize 12 types of (ZIFs) MOFs materials. When many ZIF materials were immersed in room temperature water, 50 ℃ water, boiling water and 1~7d alkaline solution, XRD analysis showed that the crystal structure of ZIF-8 and ZIF-11 remained unchanged. All tested ZIF materials can be stored in 50 ℃ water for 7 days, but only ZIF-8 can be stored in boiling water for 7 days. In addition, ZIF-8 can also be stable in sodium hydroxide solution with a concentration of 0.1~8mol/L. The MOFs of the ZIF series have good hydrothermal stability and alkaline solution stability, which benefit from the strong complexation of the divalent metal ion Zn^{2+}or Co^{2+} with the nitrogen donor of its ligand. (Park et al. 2006, 10186.)

2.2.3 Other modification methods

Carne, Stylianou & Carbonell (2015, 869-873) encapsulated the HKUST-1 material in polystyrene particles by spray drying, thereby protecting the MOFs from the influence of water and water vapor. Although the hydrophobicity of the material is improved in this way, the outer surface of the material inevitably affects the permeability of the material pores, and then affects the adsorption performance of the material. This requires precise adjustment of polystyrene and MOFs materials to obtain the best effect on adsorption capacity and hydrophobic properties. (Carne et al. 2015, 869-873)

Yang & Park (2012, 4010-4013) partially carbonized IRMOF-1 material at high temperature, and used the hydrophobicity of activated carbon formed on the surface of IRMOF-1 to increase the water stability of the material (Yang et al. 2012, 4010-4013). By accurately adjusting the carbonization conditions, the pore structure and crystal structure of the material remaining in the carbonized layer can be fully maintained, and the modified material can be stored stably in the air for one day. Certain porous materials, such as graphene and carbon nanotubes, have excellent hydrophobicity. When they are compounded with MOFs, the composite material will have a large specific surface area, excellent hydrophobicity and other properties. (Yang, Choi & Chae 2009, 1893-1897; Jayaramulu, Datta & Rcsler 2016, 1178-1182). The production of polyMOFs-organic/metal organic framework polymers by polycarboxylic acids can also improve the water stability of the materials in MOFs materials (Zhang, Nguyen & Miller 2015, 6152-6157; Zhang, Nguyen & Miller 2016, 920-925).

2.3 HKUST-1 material

HKUST-1 is a well-known MOFs material with three-dimensional pores formed by the combination of copper ions (Cu^{2+}) and trimesic acid. The Cu^{2+} node of HKUST-1 is catalytically active. In 1999, Chui, Samuel & Charmant (1999, 1148-1150) reported the structure of the porous coordination polymer HKUST-1 for the first time. This porous coordination polymer is assembled from trimellitic acid and binuclear copper clusters (FIGURE 1, left). It crystallizes in a cubic crystal system and belongs to the space group Fm-3m. It has three-dimensional open pores (FIGURE 1, right) (Chui et al. 1999, 1148-1150). Computer simulations show that HKUST-1 has excellent performance in adsorbing CO_2 and CH_4 and separating CO_2 and CH_4 mixtures. Consequently, since HKUST-1 was first reported,

increasing scientists have been studying the catalysis, separation and adsorption applications of this porous coordination polymer. (Hamon, Elsa & Pirngruber 2010, 7497-7503.)

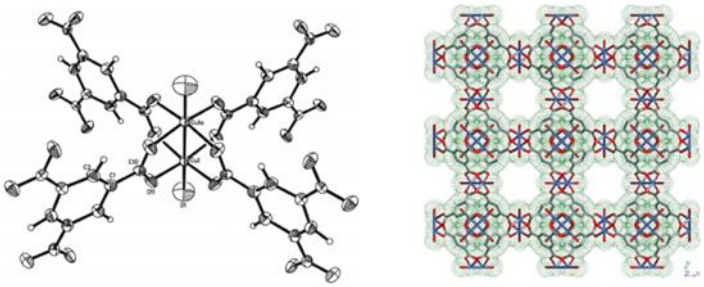

FIGURE 1. The structure of HKUST-1 (left) and three-dimensional open holes (right). (Chui et al. 1999, 1148-1150)

3 PREPARATION AND CHARACTERIZATION OF HKUST-1

The stability and adsorption properties of MOFs in humid environment were decreased obviously (Burtch et al. 2014, 10575-10612). This factor considerably affects the practical application of MOFs materials. However, through reasonable process control and material modification, the water stability and hydrophobicity of MOFs materials will be enhanced, which will be beneficial to promote the application process of MOFs materials (Mon, Bruno & Ferrando 2018, 4912-4947). This part describes the instruments and reagents used in the experiment, as well as the method and process of the experiment. The preparation, hydrophobic modification and characterization of HKUST-1 material were introduced.

3.1 Experimental reagents and Equipment

This article is an experimental paper. Below are the equipment and reagents used in the experimental part of this article. Experimental equipment includes the Sartorius electronic balance, high-speed desktop centrifuge, ultrasonic cleaning machine, magnetic heating stirrer, blast drying oven, TG analyzer, X-ray diffractometer, fully automatic specific surface and porosity analyzer, fourier transform infrared spectrometer and contact angle measuring instrument. Experimental reagents include hydrotalcite, absolute ethanol, methanol, deionized water, 1,3,5-phenyltrimetic acid, copper nitrate (II) three hydrothermal, N-N-dimethylformamide (DMF), hexadecyltrimethoxySilane ($CH_3(CH_2)_{15}Si(OCH_3)_3$).

3.2 Preparation

Up to now, as a new generation of functional materials, the research of MOFs materials have made gratifying achievements. Compared with the traditional porous material production and application process technology are more mature, but the MOFs material process technology are still in the initial stage. The stability of MOFs are not ideal enough in industrialization, so it is necessary for future researchers to design and synthesize special MOFs effectively. Therefore, there are still many practical problems to be solved in the mass production and application. Therefore, a kind of MOFs material named HKUST-1 was prepared under normal temperature and pressure. The experimental method

illustrates the specific steps and content of this experiment, including the preparation of HKUST-1 material and the hydrophobic modification of HKUST-1 material.

3.2.1 Rapid preparation of HKUST-1 material

0.1465 g of hydrotalcite powder was weighed in a beaker, and 4 mL of deionized water and 8 mL of absolute ethanol were added, it was placed in an ultrasonic cleaning machine to sonicate for 10 minutes to obtain a slurry. 0.4265 g of trimellitic acid was weighed in a beaker and 8 mL of DMF solution was added. 0.874 g of copper (II) nitrate trihydrate was weighed in a beaker and 4 mL of deionized water was added to dissolve it. The DMF solution of the above homogeneous trimellitic acid and the copper nitrate aqueous solution were added to the slurry solution. And then it was stirred in a stirrer for 1 min. The stirred liquid was poured into a centrifuge tube. The product was obtained by centrifugation (rotational speed is 8000 r/min, 5min).

The product after centrifugation was washed three times with absolute ethanol, DMF, and methanol, and soaked for 12 hours each time. The washed material was poured into a beaker and mashed to a powder. The beaker was sealed with tinfoil and many small holes were made in the surface of the tinfoil. Eventually, it was placed in a drying box and activated at 100 ℃ for 4 hours. The dried dark blue powder is HKUST-1 material.

3.2.2 Hydrophobic modification of HKUST-1 material

0.25 g of HKUST-1 material was weighed and dissolved in 5 mL of anhydrous toluene by ultrasonic at room temperature to obtain a suspension. 0.2165 g of hexadecyltrimethoxysilane was dissolved in 10 mL of anhydrous toluene, and the suspension was added with stirring. The mixture was stirred at room temperature for 24 hours at 500 rpm. The suspension was then poured into a centrifuge tube and centrifuged in a centrifuge. The solid precipitate after centrifugation was centrifuged twice with absolute ethanol. Then the solid precipitate after centrifugation was poured into a beaker and mashed into a powder. The beaker was sealed with tinfoil and many small holes were made in the surface of the tinfoil. Eventually, it was placed in a drying box and activated at 100 ℃ for 5 hours to obtain the modified HKUST-1, named HKUST-1-A.

3.3 Characterization

The term "characterization" is a term used in chemistry and materials science to describe the analysis, testing or identification of a substance by physical or chemical property and to elucidate its chemical properties. The concept includes a number of specific means, including a variety of microscopy, ultraviolet spectrum, visible spectrum, infrared spectrum, electronic spectrum, mass spectrum. The characterization features include element composition (or chemical composition), chemical environment (or bonding condition), crystal structure, surface morphology. The characterization method is to send the synthesized HKUST-1 material and the hydrophobically modified HKUST-1-A material for material characterization. Material characterization includes BET characterization, XRD characterization, TG characterization, infrared spectroscopy and contact angle measurement.

3.3.1 X-ray powder diffraction analysis (XRD)

X-ray powder diffraction (XRD) is one of the most commonly used techniques for batch analysis of powders. It can determine the phase composition and crystal structure of powder materials. Due to the crystal lattice structure, when X-rays are injected into the crystal, the scattered waves of electrons overlap and interfere with each other. Therefore, by interpreting the spectrum produced by X-rays passing through the material, one can understand the purity of the material, the crystal structure and the particle size of the crystal. In addition, X-ray powder diffraction can not only be used for the quantitative analysis of crystals, but also can accurately determine the crystal grain size, lattice constant and Miller index. (Sonibare, Haeger & Foley 2010, 5347.) The XRD analyzer used in this experiment is Rigaku, Japan, and the model of the instrument is Ultima IV. The experiment used a Cu target Kα radiation source with a wavelength of 0.1546 nm, a tube voltage of 40 kV, a tube current of 30 mA, scanning at a speed of 5°/min, and a test range of 5° to 55°.

3.3.2 Characterization of pore structure and specific surface area (BET)

The material synthesized in this experiment was measured by ASAP 2460 specific surface area analyzer for BET and pore structure. The analyzer is based on the principle of static volumetric method.

First, the material must be pretreated at 150 ℃, and then put the material into the analyzer to absorb and desorb the N_2 to obtain the N_2 adsorption and desorption curve. The instrument will use the BET equation, the Langmuir equation and the adsorption isotherm to process the experimental data on its own and get the experimental results.

3.3.3 Fourier Infrared Spectroscopy

Infrared spectroscopy is one of the important methods used to analyze substances. Through infrared spectroscopy, it is possible to understand the functional group information of the material and the structural properties of the entire material. This method is determined by analyzing the information such as the rotation and vibration of the material atoms. (Xu, Yuan & Lu 2000, 134-142.) The Fourier transform infrared spectrometer used in this experiment is made by Bruker, Germany. The focal length is 150 mm. The spectral measurement range is 7800 ~ 230 cm-1(1.5 ~ 50 μm). The resolution of the spectrometer is 0.16 cm^{-1}. The precision of micro-area measurement is 0.1 μm. And the transmission spectrum of 6.6 μm sample can be measured.

3.3.4 Thermogravimetric analysis (TG characterization)

TG analysis means that when the temperature changes, the quality of the material is recorded, and the relationship between the quality of the material and the temperature or time is obtained. The TG characterization of this experiment uses the German Netzsch STA2500 thermal analyzer. Its resolution is 0.03 μg. The vacuum is 10-4 mbar. The highest temperature can reach 1600 ℃. The hydrophobically modified HKUST-1-A material was placed in the balance of the thermal analyzer, and continue to heat up to 600 ℃ under a nitrogen atmosphere at a rate of 10 ℃/min.

3.3.5 Characterization of contact angle

The contact angle tester used in this experiment is from Germany. The contact angle reflects the affinity of the solid to the liquid, and it is a very important parameter. The contact angles of hydrophilic, hydrophobic and superhydrophobic materials are respectively less than 90°, between 90° and 150° and

greater than 150°. In the case of visible droplets, the interfacial tension of gas, liquid and solid conforms to Young's equation (1):

$$\gamma_{lv}cos\theta = \gamma_{sv} - \gamma_{sl} \qquad (1)$$

Among them, γ is the interfacial tension, the subscripts v, l, and s represent gas, liquid and solid phases, respectively, and θ is the contact angle. Drop a droplet onto the surface of a solid sample, and use a microscope lens and camera to obtain an image of the droplet shape, and then use some algorithms and digital image processing to calculate the contact angle of the image droplet.

3.4 Determination of water adsorption performance

Water absorption performance includes two parts: water absorption kinetics and diffusion coefficient. This part uses the gravimetric method to measure the amount of water adsorbed by the material. Firstly, two containers with relative humidity of 32.8% and 81% respectively were prepared. The container with a relative humidity of 32.8% was composed of magnesium chloride solution. The container with a relative humidity of 81% was composed of ammonium sulfate solution. Then the weighed HKUST-1 material and HKUST-1-A material were put into a container with a relative humidity of 32.8%. For the first 10 minutes, they were took out every 1 minute to weigh them and record the data. After 10 minutes, they were weighed every 10 minutes. The HKUST-1 material and HKUST-1-A material were weighed again into a container with a relative humidity of 32.8%. For the first 10 minutes, they were took out every 1 minute to weigh them and record the data. After 10 minutes, they were weighed every 10 minutes.

3.4.1 Water adsorption kinetics

In this experiment, the gravimetric method is used. Under the same temperature and pressure, different relative humidity, with the change of time, the adsorption amount of water on HKUST-1 and HKUST-1-A materials are measured. That is to measure the total mass of the material at different times, and then use the following formula (2) (3) to calculate the amount of water absorbed per gram of material. The different relative humidity is 81% (ammonium sulfate solution) and 32.8% (magnesium chloride solution). The formula for calculating its adsorption capacity is:

$$Q_e = \frac{1000\ (W_e - W_a)}{W_a M} \qquad (2)$$

$$Q_t = \frac{1000\ (W_t - W_a)}{W_a M} \qquad (3)$$

In the formula, M(g/mol) —relative molecular mass of water;

W_e (g) — mass when adsorption is saturated;

W_a (g) —the initial mass of the material;

W_t (g) — t (s) time material quality;

Q_e (mmol/g) — is the amount of H_2O adsorbed per gram of material in the adsorption equilibrium.

Q_t (mmol/g)—The amount of H_2O adsorbed per gram of material at t (s) time.

3.4.2 Diffusion coefficient (D_M)

The D_M reflects an important parameter of the degree of gas (or solid) diffusion. It refers to the diffusion capacity of water in the material, which can be calculated by the kinetics of water adsorption. The calculation formula (4) of D_M is (Miyoshi & Hirofumi 1999, 231-245):

$$\frac{Q_t}{Q_e} \cong \frac{6}{r_c}\sqrt{\frac{D_M t}{\pi}} \qquad (4)$$

In the above formula, r_c (cm) is the average particle radius, D_M (cm^2/s) is the D_M between crystals, and t is the time (s). Through the water adsorption curve, the value of Q_t/Q_e can be calculated, and then plot Q_t/Q_e as the y-axis and $t^{1/2}$ as the x-axis to fit a straight line and get its slope $\frac{6}{r_c}\sqrt{\frac{D_M}{\pi}}$, using this slope, the D_M and diffusion time constant (D_M/r_c^2, s^{-1}) can be obtained. The average particle radius r_c of the original material HKUST-1 and the hydrophobically modified material HKUST-1-A prepared in this paper are both 0.504 μm.

4 RESULTS AND DISCUSSION

This part deals with the data obtained from the experiment. After processing the experimental data, the origin app was used to draw a graph, and draw the XRD spectrum of the experimental material, the adsorption and desorption isotherm of the material to N_2, the infrared spectrum of the material, the TG curve of the material and the adsorption curve of the material to water. The relevant information was consulted, and the obtained results were analyzed and discussed.

4.1 Material characterization

Material characterization is a very important factor in determining materials. Material characterization is to reveal and determine the structural characteristics of materials through various physical, chemical and other testing methods. It uses the interaction of beams, electron beams or other particles with the sample to generate various information that characterizes the structural characteristics of the material, thereby obtaining rich information on the morphology, composition and structure of the material. Therefore, this is the result of material characterization determination. The following is a discussion and analysis of the results.

4.1.1 X-ray powder diffraction analysis (XRD)

Figure 2 compares the XRD spectrum of the hydrophobically modified material HKUST-1-A prepared in this paper with the original material HKUST-1 and the simulated HKUST-1. It can be seen from the XRD diagram that the main characteristic peaks of HKUST-1-A are very consistent with the main characteristic peaks of the original material HKUST-1 and the simulated HKUST-1, and the peak position and relative intensity of each peak are consistent. This shows that HKUST-1-A has high purity and strong crystallinity.

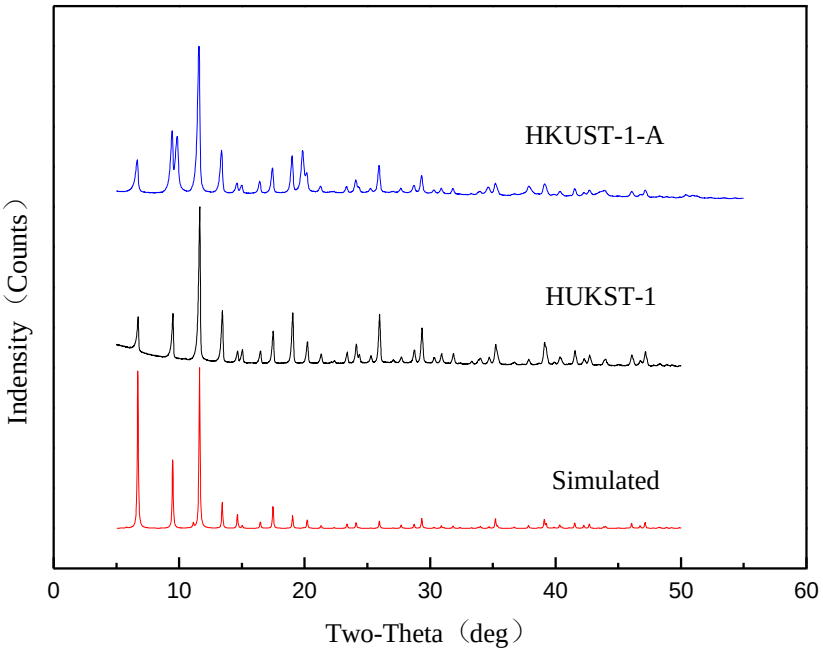

FIGURE 2. XRD spectrum of HKUST-1 crystal and its hydrophobically modified material

4.1.2 Characterization of pore structure and specific surface area (BET)

Figure 3 shows the adsorption and desorption isotherms of HKUST-1 material and hydrophobically modified material HKUST-1-A for N_2 at 350.45 ℃. When the partial pressure of N_2 is very small, the materials all show strong adsorption capacity, and the adsorption capacity for nitrogen is large; as the partial pressure of nitrogen increases, the adsorption capacity of the material for nitrogen begins to slow down, and the adsorption capacity increases very slowly. This indicates that there are abundant micropores in HKUST-1 material and the hydrophobically modified HKUST-1-A material.

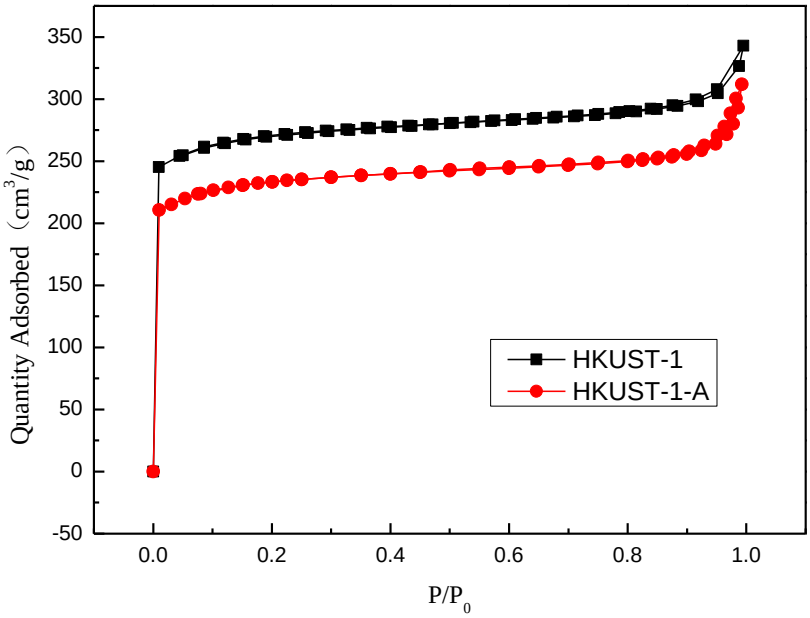

FIGURE 3. N_2 adsorption and desorption isotherms of HKUST-1 and HKUST-1-A at 350.45 ℃

Table 1 is a comparison of the pore structure of the hydrophobically modified material HKUST-1-A and the raw material HKUST-1. It can be seen from the table below that the BET of the raw material HKUST-1 is 1016.2 m^2/g, and the total pore volume is 0.530 cm^3/g; the BET of the hydrophobically modified material HKUST-1-A is 904.7 m^2/g, and the total pore volume is 0.471 cm^3/g. Compared with the raw materials, the BET and total pore volume of the hydrophobically modified materials have decreased, but the decline is not large, indicating that the hydrophobically modified materials have strong hydrophobicity while also preserving the large specific surface area and pore structure of the raw materials.

TABLE 1. Pore structure parameters of HKUST-1 and HKUST-1-A materials

Material	BET（m^2/g）	Total Pore Volume（cm^3/g）	Micro Pore Volume（cm^3/g）
HKUST-1	1016.2	0.530	0.355
HKUST-1-A	904.7	0.471	0.275

4.1.3 Fourier Infrared Spectroscopy (FTIR)

Figure 4 is the infrared absorption curve of HKUST-1 crystal and hydrophobically modified material HKUST-1-A. It can be seen from the figure that the heights of the infrared characteristic peaks of HKUST-1-A and HKUST-1 materials are consistent and basically consistent. Compared with HKUST-1 material, the peaks of HKUST-1-A are all at 2974, 1045 and 939 cm^{-1}. This indicates that the modified material is assigned to the stretching vibration of -CH; (2974 cm^{-1}), -CO (1045 cm^{-1}), and the bending vibration of the benzene ring (939 cm^{-1}), which indicates that the organic group passes through the silane Chemical effect on MOFs modified materials.

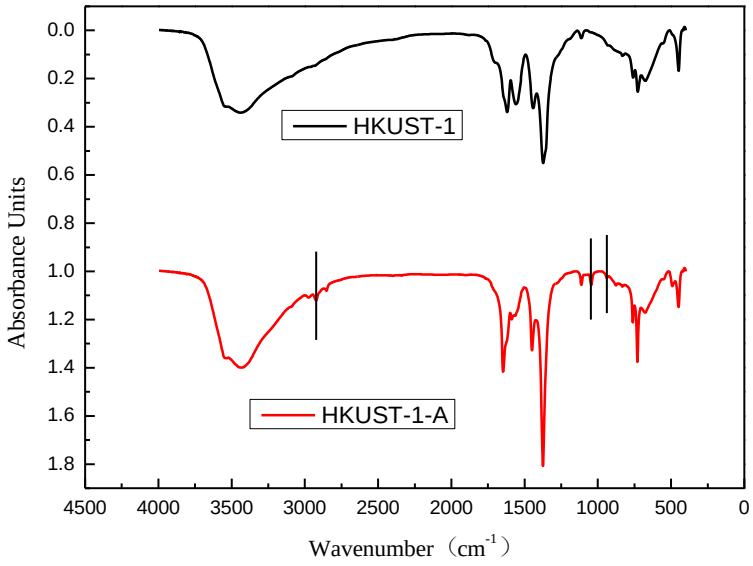

FIGURE 4. Infrared spectra of HKUST-1 crystal and HKUST-1-A

4.1.4 Thermogravimetric analysis (TG characterization)

Figure 5 is the TG analysis curve of the original material HKUST-1 and the hydrophobically modified material HKUST-1-A. It can be seen from the figure that the HKUST- and HKUST-1-A materials have two weight loss intervals. The first interval is below 130 ℃. The reason for the weight loss is that the material removes the guest molecules in the pores, and the weight loss is about 20% and 28%, respectively, which shows that the material has a very rich pore structure. The second weight loss interval is 300 ℃ to 350 ℃. The reason for the weight loss is the collapse of the internal structure of the

material. In the temperature range of 130 ℃ to 300 ℃, it is the material's removal of bound water, toluene and DMF, which indicates that the guest in the material has been completely removed, reflecting the material's better thermal stability.

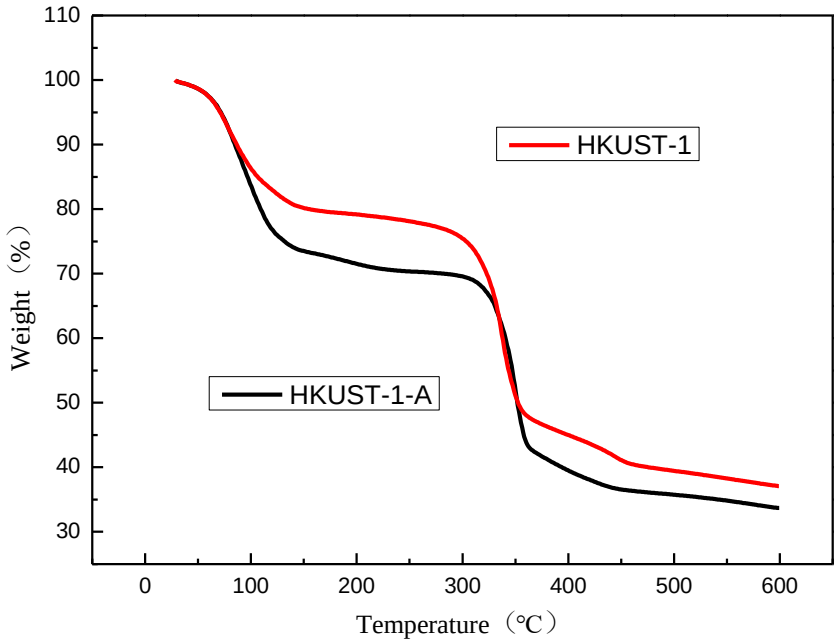

FIGURE 5. TG curve of HKUST-1 crystal and HKUST-1-A

4.1.5 Characterization of contact angle

Figure 6 is the contact angle test chart of HKUST-1-A. The larger the contact angle, the better the hydrophobic performance. It can be seen from the figure that the left contact angle of HKUST-1-A is 125.0°, and the right contact angle is 127.3°. This shows that the HKUST-1-A obtained by the hydrophobic modification of HKUST-1 with hexadecyltrimethoxysilane has strong hydrophobic properties.

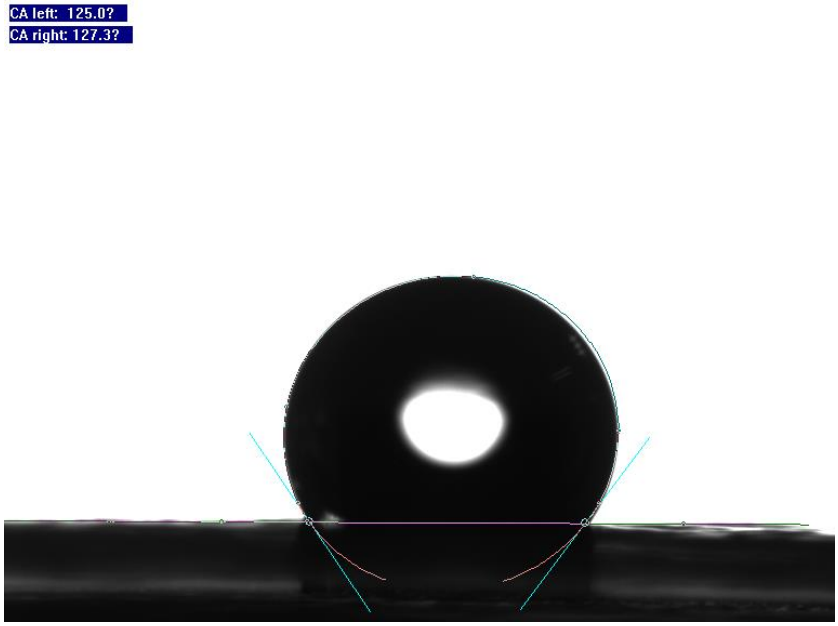

FIGURE 6. Contact angle of hydrophobically modified material HKUST-1-A

4.2 Water adsorption performance

Water adsorption performance includes two parts: water adsorption kinetics and D_M. This part is to measure the amount of water adsorbed by the material by gravimetric method. After that, the water adsorption performance results of the material are obtained through data processing.

4.2.1 Water adsorption kinetics

Figure 7 is the adsorption curves of water on HKUST-1 crystal and HKUST-1-A under different relative humidity conditions. It can be seen from the figure that as time increases, the amount of water adsorbed increases, and the adsorption reaches saturation in about 60 minutes. Under the condition of a relative humidity of 81%, the water adsorption capacity of the original material HKUST-1 is 23.7 mmol/g, while the water adsorption capacity of the hydrophobically modified material HKUST-1-A is 15.1 mmol/g, a decrease of 36.3%. Under the condition of a relative humidity of 32.8%, the water adsorption capacity before and after the hydrophobic modification of the raw material changed from 19.9 mmol/g to 14.1 mmol/g, a decrease of 29.1%.

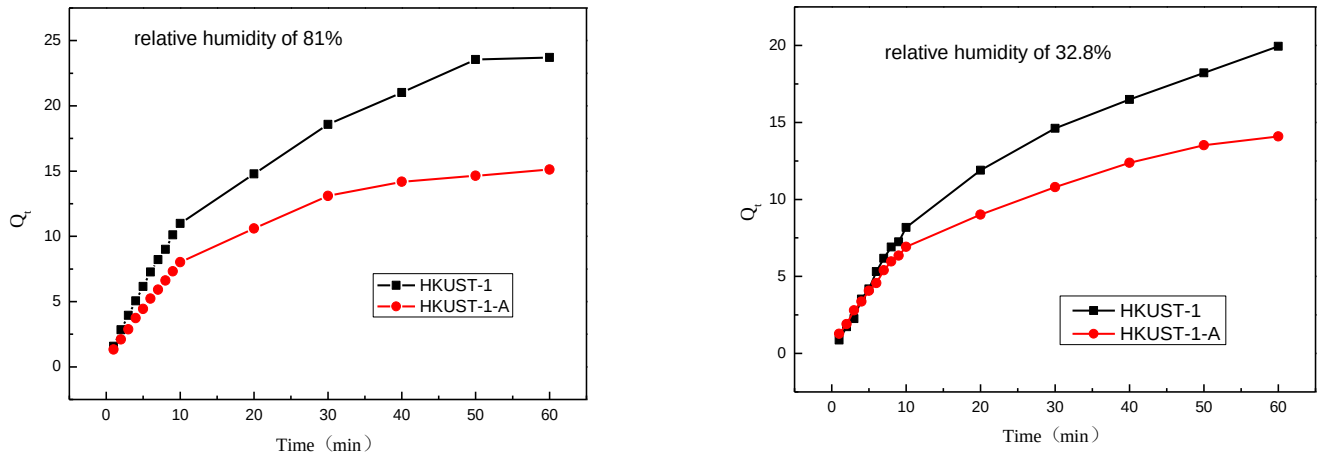

FIGURE 7. The adsorption curve of H_2O on HKUST-1 crystal and HKUST-1-A at a relative humidity of 81% and 32.8%

4.2.2 Diffusion coefficient

The D_M can reflect the diffusion performance of water in the original material HKUST-1 and the hydrophobically modified HKUST-1-A material. Therefore, the D_M can be obtained from the adsorption kinetics of water on the material. The formula (5) for calculating the D_M between crystals is as follows:

$$\frac{Q_t}{Q_e} \cong \frac{6}{r_c}\sqrt{\frac{D_M t}{\pi}} \quad (5)$$

In the above formula, r_c (cm) is the average particle radius, D_M (cm^2/s) is the D_M between crystals, and t is the time (s). Through the water adsorption curve, the value of Q_t/Q_e can be calculated, and then using the data of Q_t/Q_e <70%, plotting with Q_t/Q_e as the y-axis and $t^{1/2}$ as the x-axis, a straight line can be fitted and calculated the slope is $\frac{6}{r_c}\sqrt{\frac{D_M}{\pi}}$, which can be used to find the diffusion time constant and D_M. The average particle radius r_c of the original material HKUST-1 and the hydrophobically modified material HKUST-1-A prepared in this paper are both 0.504 μm.

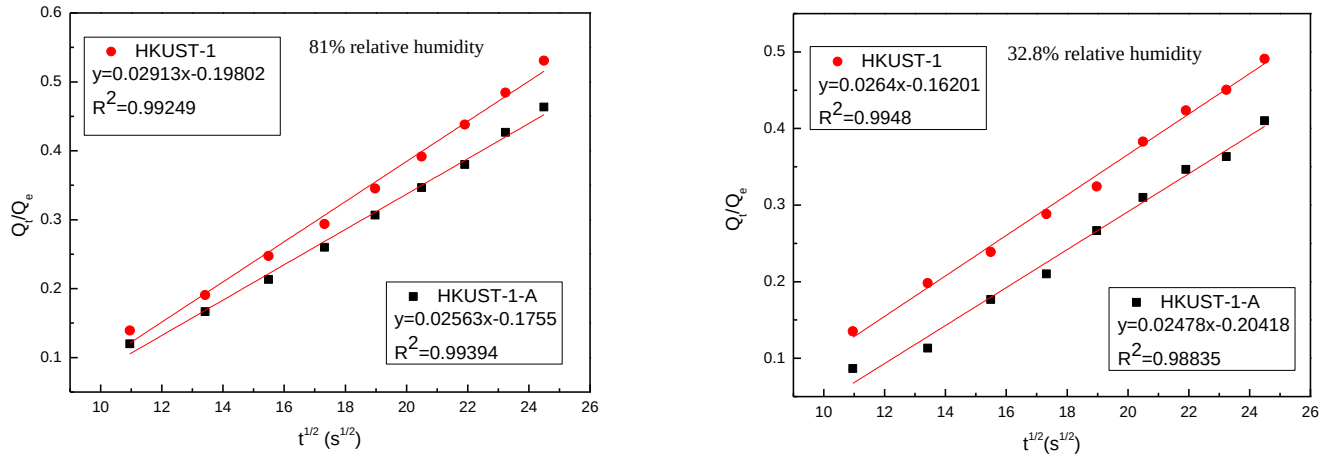

FIGURE 8. At 81% and 32.8% relative humidity, the relationship between adsorption component Q_t/Q_e and the square root of adsorption time $t^{1/2}$

Figure 8 are graphs showing the relationship between the adsorption amount of H_2O Q_t/Q_e and the time $t^{1/2}$ under the conditions of relative humidity of 81% and 32.8%, respectively. It can be seen from the figure that the linear correlation coefficients of all fitted straight lines are $R^2>0.988$. This indicates that the diffusion behavior of water vapor on HKUST-1 and HKUST-1-A materials can be well described by equation (5)

It can be seen from Table 2 that the correlation coefficient R^2 of the straight line obtained by fitting is very high. This shows that the adsorption of water vapor by the material occurs in the initial period, and the inter-crystal D_M equation (5) can describe the diffusion behavior of water vapor on the material. And, as the relative humidity increases, the slope of the straight line $\frac{6}{r_c}\sqrt{\frac{D_M}{\pi}}$ also increases. It can be concluded that the D_M is also increasing. Therefore, as the relative humidity increases, the diffusion of water vapor on the material is more favourable. Under the same relative humidity, the D_M after modification are lower than those before modification, which indicates that the diffusion of water vapor on the modified material will be slower.

TABLE 2. The model parameters of the microporous diffusion of water vapor on the HKUST-1 crystal and HKUST-1-A material particles under the relative humidity of 81% and 32.8%, respectively

Relative humidity	Material	$\frac{6}{r_c}\sqrt{\frac{D_M}{\pi}}$	$\frac{D_M}{r_c^2}$ ($\times 10^{-5} s^{-1}$)	D_M ($\times 10^{-13} cm^2/s$)	R^2
81%	HKUST-1	0.02913	7.40	1.88	0.992
81%	HKUST-1-A	0.02563	5.73	1.46	0.994
32.8%	HKUST-1	0.02640	6.08	1.54	0.995
32.8%	HKUST-1-A	0.02478	5.36	1.36	0.988

5 CONCLUSION

In general, it is feasible to use cetyltrimethoxysilane as a hydrophobic modifier to improve the hydrophobic properties of HKUST-1. Although the specific surface area and total pore volume of HKUST-materials decreased slightly after hydrophobic modification, the hydrophobic properties were considerably improved.

The first is the characterization of materials. This experiment uses hydrotalcite to quickly prepare HKUST-1 raw materials at room temperature. The BET specific surface area of the raw material is 1016.2 m^2/g, and the total pore volume is 0.530 cm^3/g. After hydrophobic modification, the specific surface area of HKUST-1-A material becomes 904.7 m^2/g, and the total pore volume becomes 0.471 cm^3/g. XRD characterization shows that the hydrophobically modified material HKUST-1-A has high purity and strong crystallinity, and also has a rich pore structure. It can be determined by TG characterization analysis that the guest molecules in the pores of HKUST-1 and HKUST-1-A can be completely removed at about 200 ℃, and they can maintain good thermal stability before 300 ℃. The contact angle characterization analysis shows that the left contact angle of the hydrophobically modified material HKUST-1-A is 125.0°, and the right contact angle is 127.3°, which indicates that the modified material has good hydrophobic properties.

The second is to study the adsorption kinetics of the material to water. The results show that under the condition of a relative humidity of 81%, the water adsorption capacity of the original material HKUST-1 is 23.7 mmol/g, and the water adsorption capacity of the hydrophobically modified HKUST-1-A material is 15.1 mmol/g, which is a decrease of 36.3%. Under the condition of a relative humidity of 32.8%, the water adsorption capacity of the original material before and after the hydrophobic modification changed from 19.9 mmol/g to 14.1 mmol/g, which is a decrease of 29.1%.

The third is to compare the D_M of water vapor in the HKUST-1 material and the hydrophobically modified material. The results show that as the relative humidity increases, the D_M increases. At a relative humidity of 81%, the D_M of water vapor on the original material HKUST-1 and the hydrophobically modified material HKUST-1-A are 1.88×10^{-13} cm^2/s and 1.46×10^{-13} cm^2/s, respectively. At a relative

humidity of 32.8%, the D_M of water vapor on the original material HKUST-1 and the hydrophobically modified material HKUST-1-A are 1.54×10^{-13} cm^2/s and 1.36×10^{-13} cm^2/s, respectively.

Therefore, after hydrophobic modification, the hydrophobic properties of HKUST-1 material are considerably improved. This shows that if the HKUST-1 material is in a humid environment, the competitive adsorption of water molecules will decrease, so its adsorption capacity for target molecules will be considerably improved. There is no doubt that it considerably improves the adsorption capacity and efficiency of MOF materials.

REFERENCES

Binnemans K. 2009. Lanthanide-Based Luminescent Hybrid Materials. Chemical Reviews 109 (9), 4283-4374.

Burtch N., Jasuja H., Walton K. 2014. Water stability and adsorption in metal-organic frameworks[J]. Chemical Reviews 114(20): 10575-10612.

Canivet J., Fateeva A., Guo Y. 2014. Water adsorption in MOFs: fundamentals and applications[J]. Chemical Society Reviews 43(16): 5594-5617.

Carne S., Stylianou K., Carbonell C. 2015. Protecting metalorganic framework crystals from hydrolytic degradation by spray-dry encapsulating them into polystyrene microspheres[J]. Advanced Materials 27(5): 869-873.

Chui S., Samuel L., Charmant J. 1999. A Chemically Functionalizable Nanoporous Material $[Cu_3(TMA)_2(H2O)_3]n$ [J]. Science 283(5405): 1148-1150.

Dhakshinamoorthy A., Li Z., Garcia H. 2018. Catalysis and photocatalysis by metal organic frameworks[J]. Chemical Society Reviews 47(22): 8134-8172.

Duan J., Jin W., Kitagawa S. 2017. Water-resistant porous coordination polymers for gas separation[J]. Coordination Chemistry Reviews 332: 48-74.

Fand X., Zong B., Mao S. 2018. Metal-organic framework-based sensors for environmental contaminant sensing[J]. Nano-Micro Letters 10(4): 64-82.

Ferey G., Mellot D., Serre C. 2005. A chromium terephthalate-based solid with unusually large pore volumes and surface area[J]. Science 309(5743): 2040-2042.

Fernandez C., Nune S., Annapureddy H. 2015. Hydrophobic and moisture-stable metal-organic frameworks[J]. Dalton Transactions 44(30): 13490-13497.

Gao C., Yang Y., Ai J. 2016. A Multifunctional Mn (Ⅱ) Phosphonate for rapid separation of methyl orange and electron-transfer photochromism[J]. Chemistry (Weinheim an der Bergstrasse, Germany) 22 (33): 11652-11659.

Guan H., Leblanc R., Xie S. 2018. Recent progress in the syntheses of mesoporous metal-organic framework materials[J]. Coordination Chemistry Reviews 369: 76-90.

Hamon L., Elsa J., Pirngruber G. 2010. CO_2 and CH_4 Separation by Adsorption Using Cu-BTC Metal Organic Framework[J]. Industrial & Engineering Chemistry Research 49(16): 7497-7503.

Howarth A., Liu Y., Li P. 2016. Chemical, thermal and mechanical stabilities of metal-organic frameworks[J]. Natural Reviews 1(3): 1-15.

Jayaramulu K., Datta K., Rcsler C. 2016. Biomimetic superhydrophobic/superoleophilic highly fluorinated graphene oxide and ZIF-8composites for oil-water separation[J]. Angewandte Chemie International Edition 55(3): 1178-1182.

Kaye S., Dailly A., Yaghi O. 2007. Impact of preparation and handling on the hydrogen storage properties of Zn_4O (1, 4-benzenedicarboxylate) (3) (MOF-5) [J]. J Am Chem Soc 129 (46): 14176-14180.

Ke F., Peng C., Zhang T. 2018. Fumarate-based metal-organic frameworks as a new platform for highly selective removal of fluoride from brick tea[J]. Scientific Reports 2018, 8 (1): 1-11.

Liu X., Li Y., Ban Y. 2013. Improvement of hydrothermal stability of zeolitic imidazolate frameworks[J]. Chemical Communications 49(80): 9140-9142.

Ma D., Lia B., Shia Z. 2018. Multi-functional sites catalysts based on post-synthetic modification of metal-organic frameworks[J]. Chinese Chemical Letters 29(6): 827-830.

Merkel T., Bondar V., Nagai K. 2000. Gas sorption, diffusion, and permeation in poly(dimethylsiloxane)[J]. Journal of Polymer Science Part B: Polymer Physics 38(3): 415-434.

Miyoshi, Hirofumi. 1999. Donnan Dialysis with Ion-Exchange Membranes. III. Diffusion Coefficients Using Ions of Different Valence[J]. Separation Science and Technology 34(2)(2): 231-245.

Mon M., Bruno R., Ferrando S. 2018. Metal-organic framework technologies for water remediation: towards a sustainable ecosystem[J]. Journal of Materials Chemistry A 6(12): 4912-4947.

Mukherjee S., Desai A., Ghosh S. 2018. Potential of metal-organic frameworks for adsorptive separation of industrially and environmentally relevant liquid mixtures[J]. Coordination Chemistry Reviews 367: 82-126.

Mustafa D., Breynaert E., Bajpe S. R. 2011. Stability improvement of $Cu_3(BTC)_2$ metal-organic frameworks under steaming conditions by encapsulation of a keggin polyoxometalate[J]. Chemical Communications 47(28): 8037-8039.

Olajire A. 2018. Synthesis chemistry of metal-organic frameworks for CO_2 capture and conversion for sustainable energy future[J]. Renewable and Sustainable Energy Reviews 92: 570-607.

Park K., Ni Z., Cote A. 2006. Exceptional chemical and thermal stability of zeolitic imidazolate frameworks[J]. Proceedings of the National Academy of Sciences of the United States of America 103(27): 10186.

Patricia H., Serre C., Vallet‐Regí M. 2006. Metal‐Organic Frameworks as Efficient Materials for Drug Delivery. Angewandte Chemie International Edition 45 (36): 5974-5978.

Pearson R. 1963. Hard and soft acids and bases[J]. Journal of the American Chemical Society 85(22): 3533-3539.

Simon Y., Mielcarek A., Couvreur P. 2018. Nanoparticles of metal-organic frameworks: on the road to in vivo efficacy in biomedicine[J]. Advanced Materials 30(37): 1707365.

Sonibare O. O., Haeger T., Foley S. F.2010. Energy (Oxford) 35(12):5347.

Sun Q., He H., Gao W. 2016. Imparting amphiphobicity on single-crystalline porous materials[J]. Nature Communications 7: 13300.

Taddei M., Costantino F., Vivani R. 2016. Robust metal-organic frameworks based on tritopic phosphonoaromatic ligands[J]. European Journal of Inorganic Chemistry 27: 4300-4309.

Wang H., Li J., Li J. 2017. Lanthanide-based metal-organic framework nanosheets with unique fluorescence quenching properties for two-color intracellular adenosine imaging in living cells[J]. Npg Asia Materials 9 (3): 1-9.

Wang H., Lustig W., Li J. 2018. Sensing and capture of toxic and hazardous gases and vapors by metal-organic frameworks[J]. Chemical Society Reviews 47(13): 4729-4756.

Wang S., Mcguirk C., Aquino A. 2018. Metal-organic framework nanoparticles[J]. Advanced Materials 30(37): 1800202.

Xu G., Yuan H, Lu W. Progress in modern near-infrared spectroscopy and its application [J]. Spectroscopy and Spectral Analysis, 2000, (02): 134-142.

Yang C, Kaipa U., Mather Q. 2011. Fluorous metal organic frameworks with superior adsorption and hydrophobic properties toward oil spill cleanup and hydrocarbon storage[J]. Journal of the American Chemical Society 133(45): 18094-18097.

Yang S., Choi J., Chae H. 2009. Preparation and enhanced hydrostability and hydrogen storage capacity of CNT@MOF-5hybrid composite[J]. Chemistry of Materials 21(9): 1893-1897.

Yang S., Park C. 2012. Preparation of highly moisture-resistant black-colored metal organic frameworks[J]. Advanced Materials 24(29): 4010-4013.

Yu J., Balbuena P. 2015. How impurities affect CO_2 capture in metal-organic frameworks modified with different functional groups[J]. Acs Sustainable Chemistry & Engineering 3 (1): 117-124.

Zhang C., Wang B., Li W. 2017. Conversion of invisible metal-organic frameworks to luminescent perovskite nanocrystals for confidential information encryption and decryption[J]. Nature Communications 8 (1): 1-9.

Zhang J., Gao G. 2018. Preparation and application of metal organic frameworks porous materials [J]. Modern Chemical Industry 38(11): 53-57.

Zhang W., Hu Y., Ge J. 2014. A facile and general coating approach to moisture/water-resistant metal-organic frameworks with intact porosity[J]. Journal of the American Chemical Society 136(49): 16978-16981.

Zhang Y. 2021. Research progress on hydrophobic modification of metal organic framework materials[J]. Chemical New Materials 49(01):61-66.

Zhang Z, Nguyen H, Miller S, et al. Polymer-metal-organic frameworks (polyMOFs) as water tolerant materials for selective carbon dioxide separations[J]. Journal of the A-merican Chemical Society, 2016, 138(3): 920-925.

Zhang Z, Nguyen H, Miller S, et al. Poly MOFs: a class of interconvertible polymer-metal-organic-framework hybrid materials[J]. Angewandte Chemie International Edition, 2015, 54(21): 6152-6157.